Diffusion kurtosis imaging (DKI) in characterization in indetermined solitary pulmonary nodules (SPNs): comparison with conventional DWI and quantitative

Zikai Li, Yi Liang, Wenhui Fan, Hanlin Wang

General Hospital of the Yangtze River Shipping•Wuhan Brain Hospital, Wuhan, 430014, Hubei, China

Introduction. To better clarify the role of diffusion kurtosis imaging (DKI) in determining the characterization of isolated pulmonary nodules (SPNs), we compared conventional DWI with quantitative imaging.

Methods. In this paper, From March 2018 to July 2020, forty-seven consecutive patients (30 male, 17 female, median age: 61 years; range: 29 to 86 years) with SPNs were included. Multi-b factor DWI (with b values from 0 to 2000 sec/mm2) and quantitative DCE-MRI data were acquired. ADC, Kapp, Dapp, Ktrans, Kep, Ve and iAUC values were compared between malignant and benign group and among subtypes of LC. The ROC curves were establishd to assess the diagnostic value.

Results. Kapp, Ktrans, Ve and iAUC values were obviously higher for malignant SPNs compared to that of benign SPNs ($P < 0.035$). ADC was obviously higher in benignity compared to malignant SPNs ($P = 0.001$). There exist no obvious difference in Dapp and Kep between the two groups ($P = 0.06$). Kapp value has highest sensitivity (81.8%) and accuracy (75.7%), and ADC value has highest specificity (80.0%). Combination of ADC and iAUC enhanced the sensitivity to 81.8%, specificity to 86.7% and precision to 83.8%.

Keywords. Diffusion kurtosis imaging, Solitary pulmonary nodules, DWI; Quantitative imaging

INTRODUCTION

Lung cancer (LC) is characterized by high morbidity and highest mortality. Many patients are already at an advanced stage when diagnosed, which caused the 5-year survival rate is only 18%[1] . LC usually presents as solitary pulmonary nodules (SPNs). SPNs are frequently detected on CT examinations in clinical practice and on low-dose CT for lung cancer screening, which helps to reduce mortality from LC [2].Therefore, the discrimination of SPNs has become an important issue for clinical management. CT and PET/CT are commonly used to differentiate SPNs, but it is difficult to avoid false positives [3-5] (active granulomas, hyper-vascular benign tumors, etc.) and false negative outcomes [3,6](various neuroendocrine tumors, highly differentiated adenocarcinomas, etc.), so the differentiation of SPNs remains a challenge. To date, MRI technology were increasingly used in lung diseases [7] and is particularly valuable in diagnosing the nature of lung tumors and nodules, dynamic contrast-enhanced MRI (DCE-MRI) and DWI are mainly used for the diagnosis of SPNs[8].

Water molecules are assumed to fit a Gaussian diffusion (free and unrestricted diffusion) in conventional DWI techniques. Thus, the DWI signal decreases mono-exponentially with increasing b value. In fact, water in body tissues does not diffuse according to a Gaussian distribution because the cell membrane or the space inside and outside the cell limits the free movement of water protons [9-10].Moreover, some cases such as lung abscess, tuberculoma, and other inflammatory or infectious foci have been reported to overlap with lung cancer in DWI. Diffusion kurtosis imaging (DKI) was first defined by Jensen et al [11], and it accurately characterizes some properties of non-Gaussian diffusion caused by complex microstructures, thus

providing a more accurate assessment of tissue microstructure than DWI. DKI was mainly used in cerebral diseases[12-13] . Up to date, the applications of DKI have been successfully extended from brain to other tissues, such as liver[14], skeletal muscle[15], breast[16] and prostate[17],due to technical progress. Related studies have shown that DKI metrics are highly correlated with tumor grade and have a higher specificity than conventional DWI in cancer diagnosis [18, 19].

DCE-MRI has become an important MRI protocol in differentiating benign and malignant SPNs to add further diagnostic specificity[20].Quantitative DCE-MRI using pharmacokinetic models enables quantitative analysis of the vasculature of SPNs and show promise in differentiating benign SPNs from malignant ones[21].

However, it is unclear whether DKI is superior to conventional DWI and DCE-MRI in distinguishing LCs from benign SPNs, and whether the combined test will improve the diagnostic rate. Our study aims to research the diagnostic value of DKI relative to conventional DWI and DCE-MRI for SPNs and to clarify the association between diffusion and perfusion parameters.

MATERIALS AND METHODS

Patients

Informed consent was got from research objects and approved by the ethics committee of our hospital . A total of 66 patients with undiagnosed SPNs who attended our hospital from March 2018 to July 2020 were included.The SPNs indeterminacy was determined by two senior chest radiologists who has experience in pulmonary nodules diagnosis over 20 years by CT on consensus. Enrollment criteria included the followings: (a) all nodules were measured on MSCT according to RECIST criteria (version 1.1)[22] and the longest axis diameter was 8mm-30mm; (b)

all patients were pathologically confirmed; (c) nature of SPNs was determined by pathological diagnosis within 2 weeks after MRI; (d) no prior treatment before MRI. Among them, nineteen cases were excluded duo to following causes: patients who had not undergone surgery or biopsy (n=16), poor imaging quality due to various reasons (n = 1), and contraindications of MR scan or contrast administration (n=2).

Finally, up to 47 subjects were included . 30 males and 17 females with a median age of 61 years (29 to 86 years). The median age for males and females was 62,55 years, respectively.The pathological results were obtained by lobectomy in 42 cases (89.4%) and CT-guided biopsy in 3 patients (6.4%). 2 cases (4.2%) were determined by CT follow up that showed absorbed lesions.

MR Imaging acquisition

MR scans were performed on a 3.0 Tesla (T) 16-channel MR scanner (Magnetom Skyra syngo, Siemens Healthcare, Germany).The MR plain scan included HASTE T2-weighted imaging ([TR]=1100 ms, echo time [TE]=87 ms, field of view [FOV]= 360 × 360 mm^2, [TA] = 35 s, thickness = 6.0 mm), transverse VIBE T1 weighted imaging (TR/TE=4.42ms/2.46ms, FOV=360×360mm^2, matrix=256×256, TA=16 sec, slice thickness=3.0 mm) and axial respiratory triggered fat-suppressed BLADE T2-weighted imaging (TR/TE=3000ms/83ms, FOV=360×360mm^2, matrix=320×320, TA=1 min 50 sec, slice thickness=5.0 mm). Multi-b factor fat suppressed diffusion weighted imaging (DWI) acquisition of DWI and DKI data using the single-shot echo planer imaging (SS-EPI) technique was performed with 7 b-values (0, 50, 200-2000 s/mm^2)in the respiratory-triggered mode (TR/TE=2000ms/66ms; FOV= 340 cm; GRAPPA 2; maximum NEX of 10 and 24 sections, 3 orthogonal directions of X,Y and Z).

The DCE-MRI protocol consists of fast dynamic MR acquisition and multi-flip

angle T1 mapping.Same parameters (TR/TE, thickness, FOV, etc.) for both sequences.Multi-flip angle T1 mapping with three flip angles (TR/TE=2.63/1.02ms, FOV=320×320mm^2, matrix=320×320, TA=11-19 sec, thickness=4 mm, no gap, flip angles 2°/9°/12°). Then a TWIST-VIBE sequence based dynamic contrast enhanced scan with 65 phases was employed (TA=5min 33sec, thickness=4mm, no gap, flip angles 6°, temporal resolution=3.0 s/phase). Patients were scanned during each breath-hold of 12sec for 4 phases, followed by a 6-sec free breath. Finally, gadobiamide (Omniscan; GE Healthcare, WI) was rapidly injected with dose of 0.1 mmol/kg body weight (2.5 mL/sec) followed by 20 mL of saline (2.5 mL/sec).

Post-processing of MR data

All DKI data were processed by using prototype software(MR body diffusion Toolbox version 1.3, Siemens healthcare, Germany).The calculation of DKI parameters were derived from the five b-values (0, 400, 800, 1400, and 2000s/mm^2) according to the formula: $S(b) = S_0 \cdot exp\,(-b \cdot \text{Dapp} + 1/6 \cdot b^2 \cdot \text{Dapp}^2 \cdot \text{Kapp})$, in which S(b) and S0 refer to the signal intensity . Apparent diffusion coefficient Dapp (unit: ×10-3mm2/s), corrected to simulate non-Gaussian behavior.Kapp(the apparent kurtosis coefficient) ,a dimensionless parameter(unitless), represented the apparent diffusional kurtosis which may highlight cellular microstructural properties by digitally simulating intracellular barriers and compartments [23]. The ADC was calculated using the above software following the equation S(b) = S0.exp (-b.ADC) for five b values of 0, 50, 200, 400 and 800 s/mm^2.Two radiologists were blinded to the pathologic results, performed the data analysis and parameter measurements independently. Trace the solid part of the nodule in the ADC map, draw a region of interest (ROI) around the solid part and copy it to the Kapp and Dapp maps. The operation is performed three times and the average of the obtained results is

calculated.

The DCE-MRI data were processed by software Tissue 4D (Siemens Healthcare, Erlangen, Germany). The software is set to automatic mode and motion correction is performed internally and registered for use. Adjust to Tofts model mode and enter data to calculate the relevant parameters for pharmacokinetics. It was then adjusted to Arterial Input Function (AIF) mode, with the type selected as "intermediate" and located in the descending aorta on the same layer of the nodules. Perfusion parameters for ROI were subsequently obtained, including Ktrans, iAUC, Kep, and Ve. ktrans represents the transfer constant of the substance as it crosses the endothelium; iAUC refers to the area under the concentration curve within 1 minute of gadolinium concentration injection. kep refers to the transfer rate of the contrast agent and represents the shuttling ability of the contrast agent in the extracellular extravascular space (EES) or plasma;

Statistical Analysis

Data were analyzed based on SPSS 19.0 statistical software .The measurement datas are described as mean ± standard deviation. The normality and homogeneity of the data were tested. The t-test was applied for comparison between groups of data of meeting normal distribution, and the nonparametric test was applie to check the none normal distribution variables. According to DeLong et al [24], ROC curves were applied to evaluate the value of variable in differentiating benign and malignant SPNs. The diagnostic efficacy of each parameter was expressed as the AUC.

The interobserver agreement of the measurements was evaluated based on the interclass correlation coefficient (ICC).ICC > 0.75 was considered to be a high agreement [25].The relationship between the parameters was checked based on Pearson correlation test and expressed as correlation coefficient (r). $0.75 < r < 1.00$, high; 0.50

< r < 0.74, moderate ; 0.25 < r < 0.49, low correlation; r < 0.49, no correlation [18]. $P < 0.05$ was considered significantly difference.

RESULTS

Pathologic Findings

Of the 47 SPNs,30(63.8%) were male (median age, 61years; range, 29–86 years) and 17(36.2%) were female (median age, 55 years; range, 39–70 years), 28(59.5%) were malignant and 19(40.6%) were benign. The malignant SPNs included squamous cell carcinoma (n = 4), adenocarcinoma (n=19), adenosquamous carcinoma (n=2), small cell lung cancer (SCLC) (n=1) and metastasis (n=2). Benign SPNs included tuberculous granuloma (n = 9), chronic inflammatory granuloma (n=4), organized pneumonia (n=2), active infection (n=2), chondroma (n=1) and aspergilloma (n=1).

Comparison of DWI, DKI and DCE-MRI metrics between two group SPNs

The interobsever correlation coefficients(ICC) between reader 1 and reader 2's measurements of ADC, Kapp, Dapp, Ktrans, Kep, Ve and iAUC were[0.967(95%CI: 0.936, 0.983), 0.939(95%CI: 0.882, 0.969), 0.790(95%CI: 0.593, 0.892), 0.963(95%CI: 0.906, 0.986), 0.934(95%CI: 0.883, 0.969), 0.917(95%CI: 0.879, 0.946), 0.958(95%CI: 0.926, 0.982)].The ICC indicated a good to excellent agreements. In the following analysis, reader1's measurements were used for data analysis.

The mean Kapp, Ktrans, Ve and iAUC values were obviously higher in malignant SPNs compared to that in benign ones (P<0.05).The mean Kapp, Ktrans, Ve and iAUC values for malignant and benign SPNs were 0.83±0.200 Vs 0.69±0.108(P=0.018), 0.44±0.273 Vs 0.27±0.198(P=0.034), 0.38±0.252 Vs

0.25±0.119(P=0.034) and 20.11±13,278 Vs 10,02±6.258(P=0.006). The ADC values were significantly lower (1.27±0.216×$10^{-3}$$mm^2$/s) for LC than those for benign SPNs (1.60±0.357×$10^{-3}$$mm^2$/s). Dapp and Kep values were found to be have no obvious difference between the two group(P=0.908 and P=0.988,respectively). See Table 1 and Figure 1 for details.

Table 1 Comparison of DWI, DKI and DCE-MR parameters between two group SPNs

	Malignant	Benign	t/z	P value
ADC(×10−3mm2/s)	1.27±0.216	1.60±0.357	-3.482	0.001*
Kapp	0.83±0.200	0.69±0.108	2.478	0.018*
Dapp(×10−3mm2/s)	2.14±0.826	2.11±0.698	0.116	0.908
Ktrans(min-1)	0.44±0.273	0.27±0.198	2.119	0.034*
Kep(min-1)	2.12±2.108	1.79±1.380	0.015	0.988
Ve	0.38±0.252	0.25±0.119	2.206	0.034*
iAUC(mmol.kg-1.s)	20.11±13.278	10.02±6.258	2.769	0.006*

Note.—in general, data are m ± SD.
t/z represents statistics value.
* means obvious difference between two group.
P value represents the significance between the two group.

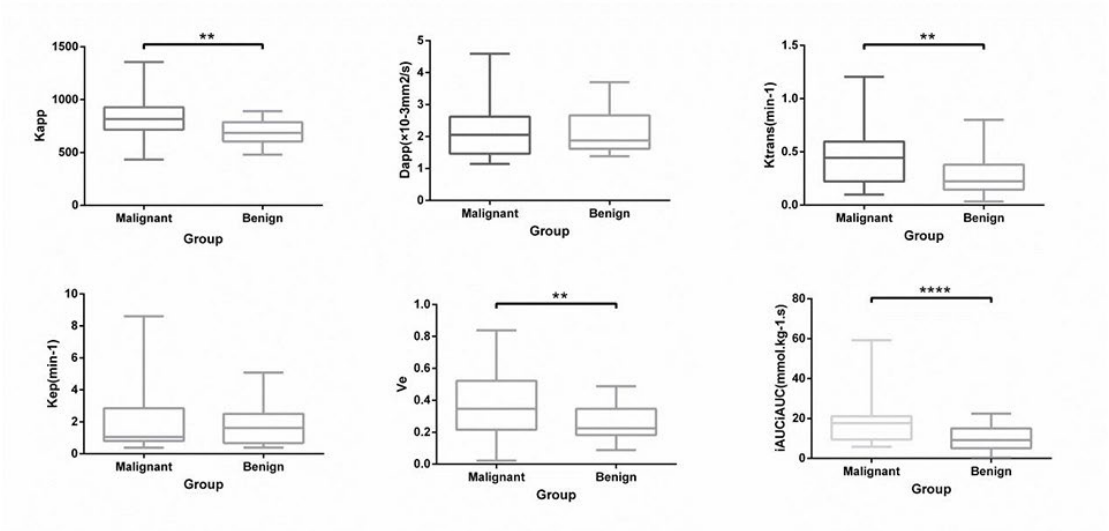

Figure 1 Box plot of multi parameters in malignant and benign SPNs group.(**means P <0.05,****means P <0.01)

All this parameters were also compared among subtypes of lung cancer and benign SPNs. Compared to benign SPN,the adenocarcinoma had higher Kapp values and

lower ADC values. There were no differences in other parameters between the three methods. See Table 2.

Table 2 Comparison of DWI,DKI and DCE-MR parameters between subtypes of lung cancer and benign SPNs

	Squamous cell carcinoma	Adenocarcinoma	Benign	P value
ADC(×10−3mm2/s)	1.32±0.254	1.23±0.212a	1.60±0.357a	0.012a
Kapp	0.81±0.157	0.87±0.199a	0.69±0.108a	0.016a
Dapp(×10−3mm2/s)	2.15±0.662	2.02±0.645	2.11±0.698	0.416
Ktrans(min-1)	0.49±0.47	0.43±0.208	0.27±0.198	0.236
Kep(min-1)	3.44±3.478	1.74±1.508	1.79±1.380	0.314
Ve	0.30±0.240	0.40±0.209	0.25±0.119	0.136
iAUC(mmol.kg-1.s)	18.26±22.963	21.67±9.984	10.02±6.258	0.052

Note.—in general, data are m ± SD.

a means significant difference between adenocarcinoma and benign group.

P value represents the significance between groups

Diagnosis performance of DWI, DKI and DCE-MRI metrics between malignant and benign SPNs

Kapp value has highest sensitivity (81.8%) and accuracy (75.7%), ADC value has highest specificity (80.0%) and equal accuracy as Kapp. Combination of ADC and

iAUC enhanced the sensitivity to 81.8%, specificity to 86.7% and precision to 83.8%. See Figure 2. Representative example is shown in Figure 3-4.

Figure 2 ROC curves of multi parameters in diagnosis of SPNs.

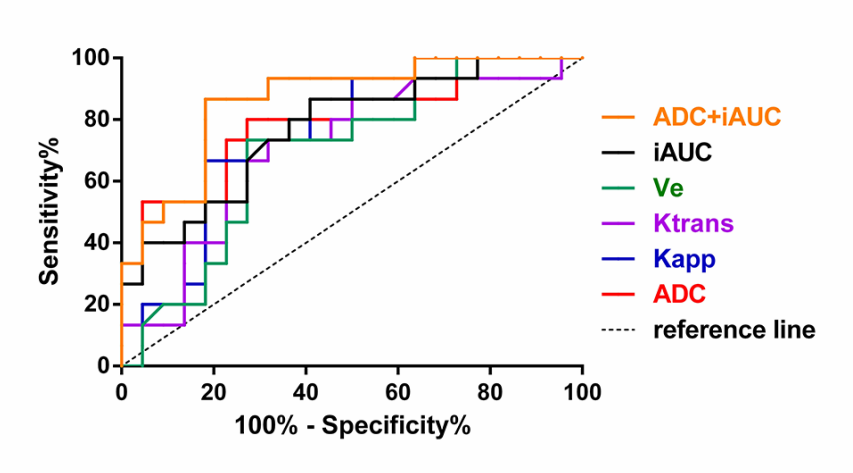

Figure 3 Representative case of a low to moderately differentiated adenocarcinoma (arrow) in the right upper lobe of lung of a 61-year-old male case. (a) Axi T2-weighted MR image shows the tumor (arrow) in the posterior segment of right upper lobe.(b-e) multi-b factor diffusion weighted imaging, b=400,800,1400 and 2000 s/mm2 ,respectively. (f)Kapp map of the SPN, Kapp value=0.74. (g)Dapp map of the SPN, Dapp value=1.76 mm2/s. (h) DCE-MR imaging of one phase shows moderate homogenous enhancement of the nodule. (i) Ktrans map, Ktrans=0.506 min-1.(j) iAUC map, iAUC=18.43 mmol.kg^{-1}.s

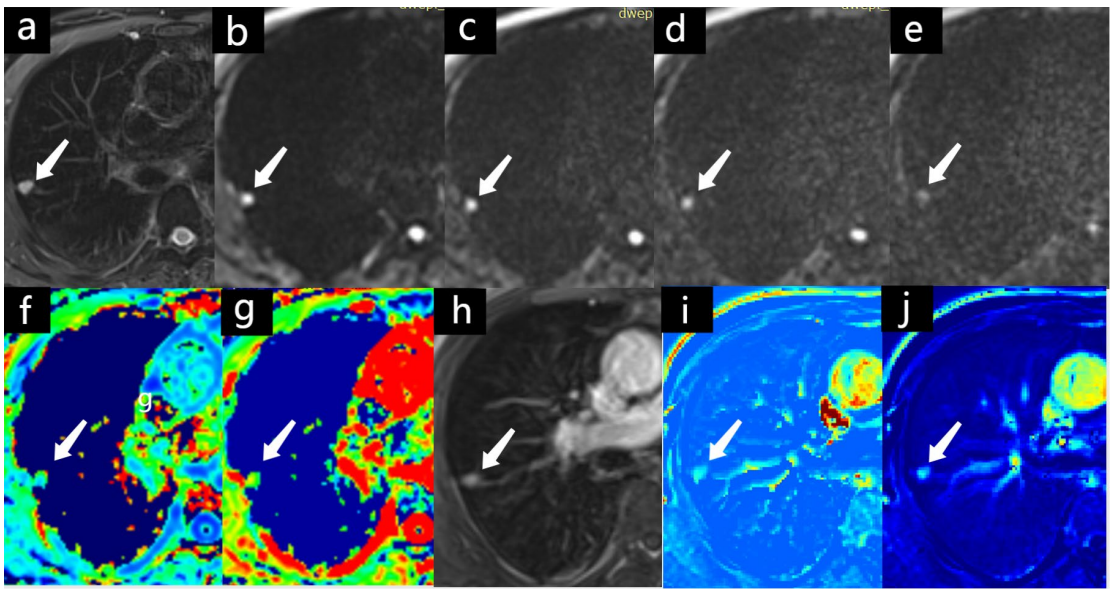

Correlation analyses of parameters derived from diffusion imaging and quantitative

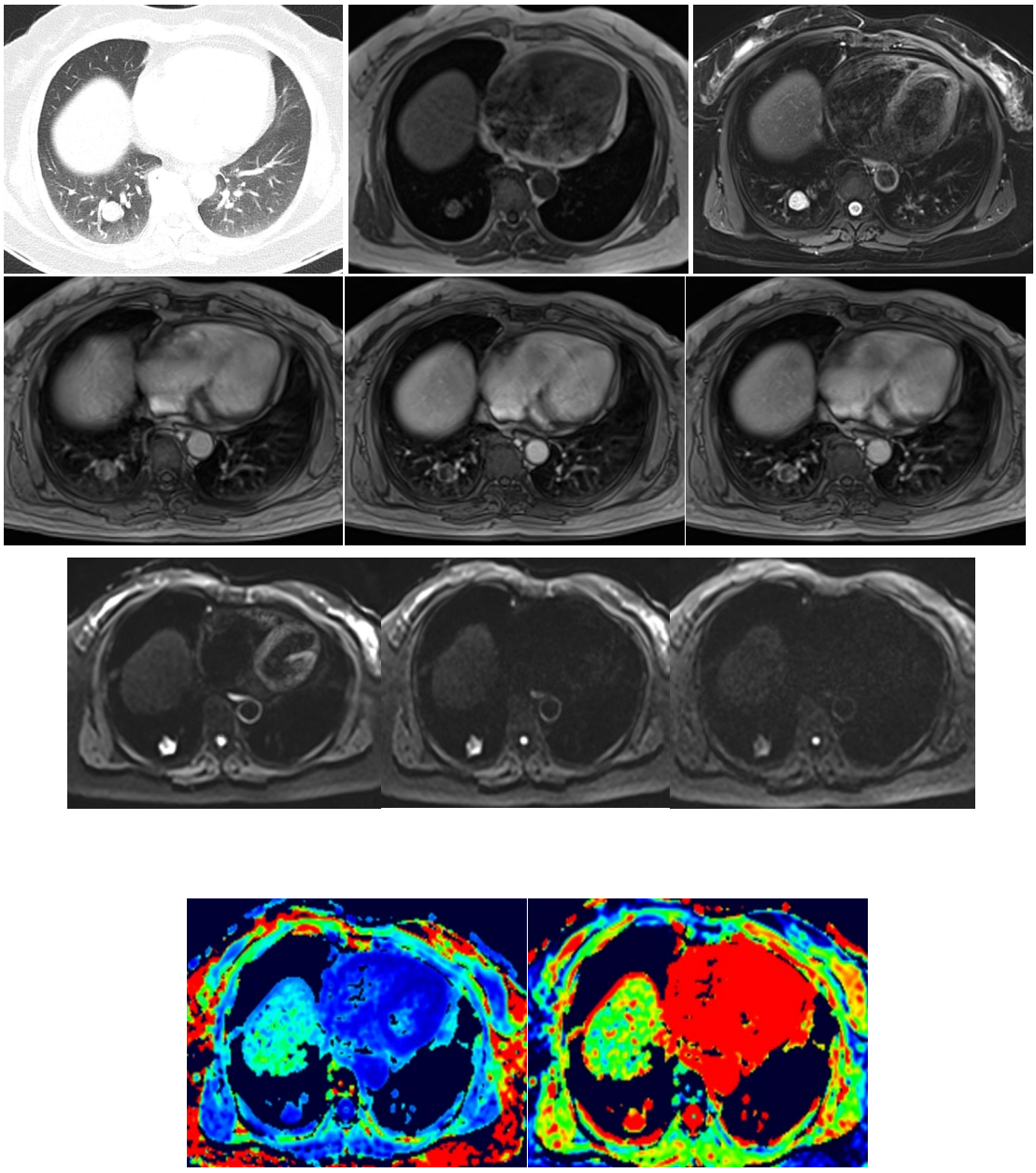

Figure 4 Female 63-year-old right lower lung nodule 4 years after surgery Pathology: sclerosing hemangioma(a). CT plain scan lung window, the size of the right lower lung is about 16.8mm × 17.3mm solitary pulmonary nodule.(b). MR plain scan T1WI and T2WI axis bitmap.(c-e) Axis bitmap of 30s, 1min and 4min during DCE-MRI scanning.(f-h) b=4008002000 s/mm2 diffusion weighted diagram.(i) Kapp pseudo-color map, Kapp=0.83.(j) Dapp pseudo-color image, Dapp=2.32 mm2/s

DCE-MRI

No significant correlation was found between the parameters of quantitative DCE-MRI and diffusion imaging, can be seen from Table 3.

Table 3 Correlation of Parameters Derived From Diffusion Imaging and Quantitative DCE-MRI

		Ktrans	Kep	Ve	iAUC
ADC($\times10^{-3}mm^2/s$)	r	-0.060	-0.141	-0.299	-0.273
	P	0.726	0.405	0.072	0.102
Kapp	R	-0.126	-0.084	0.204	0.124
	P	0.456	0.621	0.226	0.465
Dapp($\times10^{-3}mm^2/s$)	R	0.042	0.193	-0.187	-0.300
	P	0.807	0.252	0.267	0.072

DISCUSSION

Solitary pulmonary nodules refer to solitary round or quasi-circular nodules in the lung parenchyma with the largest diameter of no more than 3cm, and are not accompanied by hilar and mediastinal lymph node enlargement, atelectasis or pneumonia and other diseases. At present, high-resolution spiral CT is the main method for the differential diagnosis of solitary pulmonary nodules, but it can only speculate the pathological nature of the lesions by analyzing the morphological characteristics of the nodules (location, shape, size, number, density, edge, internal structure and the impact on the surrounding structure, etc.). Therefore, CT has certain limitations in differentiating various solitary pulmonary nodules. PET/CT is considered to be the most widely used imaging method for the evaluation of tumor metabolic status at present. However, it is sometimes difficult to distinguish inflammatory lesions and malignant tumors, and its high cost and high examination cost limit its universal application. MRI can not only provide the information of lesion morphology, but also provide the information of function, physiology,

pathophysiology and molecular aspects. Based on the progress of computer science, medical electronics, physics and other disciplines, MRI gradually overcomes the problems of soft tissue-gas interface magnetic sensitive artifacts, respiratory motion artifacts and cardiac pulsation artifacts, long scanning time , high field strength Ultra-high field magnetic resonance scanners are more and more widely used in chest imaging, making the imaging diagnosis of solitary pulmonary nodules develop from simple morphological imaging to functional imaging.

This study investigated and calculated DWI, DKI and DCE-MRI parameters of SPNs with different properties, and compared the differences of each parameter between benign and malignant SPNs and between LC subtypes. The results showed the important clinical value of the three methods for the identification of the nature of SPNs.The three methods have similar differentiation diagnosis performance between benign versus malignant SPNs. Moreover, ADC value derived from DWI, along with the iAUC values derived from DCE-MRI, with high accuracy in distinguishing benign and malignant SPNs, and has outstanding sensitivity and specificity.

DWI has been reported to be a predictive parameter of tumor cell load and heterogeneity[26].Previous study of DWI in lung lesion differentiation reported ambiguous conclusions, for instance, several clinical studies have shown that the ADC values of benign SPNs do not differ from those of lung cancer [27-28]. liu et al [29] showed that the ADC values of benign SPNs were larger compared to those of lung cancer and that the ADC had a high value in predicting the nature of SPNs (sensitivity, 83.3%; specificity, 74.1%).The accuracy of the measurement of ADC values is related to the number of b-values incorporated. The accuracy increases with the number of incorporated b-values [30].In this study, a serial of 5 b values (0, 50, 200, 400, and

800s/mm2) were used to calculate the ADC value to make the parameter more accurate. Also, excellent interobserver agreements were found in ADC value. It verified the ADC value is a stable and repeatable parameter in SPN differentiation. The benign group was found to have higher AD values than the lung cancer, similar to some previous studies[29], indicating the hypercellularity, packed cell nucleus and decreased extracellular space and hence restricted water molecule diffusion in tumor tissues.

In 2005, Jensen et al[31] proposed the DKI model for the first time. Through multi-parameter quantitative analysis of the diffusion characteristics of non-Gaussian distribution of water molecules in the organization, it is highly sensitive to the irregular diffusion of water molecules, and obtains more accurate diffusion information, so as to more truly reflect the complexity of the organization's microstructure environment. Due to the particularity of the lung, there are few clinical studies of DKI in the lung.

According to a previous study [23], there are certain rules for setting the b-value of DKI. To obtain the best kurtosis imaging, one b-value is set higher than 1000s/mm^2 and the other b-value is lower than 1000s/mm^2, b-values do not exceed a maximum of 1500-2000s/mm^2, a condition to effectively observe non-Gaussian behavior, but avoid violation of assumptions of the DKI model[32]. In addition, the minimum b value can be 0. Intravoxel incoherent motion (IVIM) often interferes with the results, and in this case we can set the minimum b value to ≥200s/mm^2 to eliminate its perfusion effect. Given the importance of SNR for high b value diffusion image, high NEX(number of excitation) and relative low spatial resolution was applied to improve the SNR at high b value image, thus to get more accurate kurtosis parameters. Since holding the breath interferes with the SNR of DWI [33] and affects the results, breathing triggering was

used in this study. A previous study [34] pointed out that the diffusion tensor enables multidimensional manipulation of DKI. In the study of tumors, the number of b-values is limited, so only 3 directions of DKI operations are required [31].Take all the above consideration, multi b values (0, 400, 800, 1400, and 2000s/mm^2) with the largest NEX of 10, 3 orthogonal directions were taken to analyze DKI data.

Heusch et al[35] performed PET/CT, PET/MRI and chest DKI on 15 NSCLC case, and selected 5 b values respectively. The results showed that the parameters of DWI and DKI were correlated with SUVmax, which was classified as ADCmono: R=-0.67, P<0.01;Kapp：R =0.72，P ＜0.05； All parameters are also correlated with SUVmean, respectively ADCmono: R=-0.66, P<0.01； Kapp：R =0.71，P＜0.005。It proves the feasibility of DKI in lung research.

In this study, the Kapp and Dapp values of lung cancer and benign SPNs were compared. There exist no obvious in Dapp values between the two groups, while Kapp values were high in lung cancer patients. This finding suggests that the diffusion of lung cancer tends to have a non-Gaussian distribution, while benign SPNs tend to have a Gaussian distribution. In agreement with the results of Das SK et al [36]. Kapp has a high specificity for detecting cellular microstructures. It not only indirectly reflects the distribution of interfaces within cells and tissues, but also refracts the interactions of water within cells and tissues [23, 32]. Except for heavier cell load, elevated nucleus-cytoplasma ratio, tumor tissues often have distortion of extracellular space, immature tumor angiogenesis, and devastation of normal cellular framework, all these factors may lead to increased Kapp value in malignant SPNs. Theoretically, a correction to Dapp is applied as a diffusion coefficient given the effect of non-Gaussian behavior. When the value of b is balanced, the intensity decay is plotted according to the variation of the diffusion signal, with Dapp as the slope [23].It is

speculated that Dapp is more accurate than conventional ADC value. However, no obvious differences were found of Dapp value between two groups in the present study, the result is different from previous study of breast lesions[18].The reason cannot be well interpreted and need further evaluation with larger sample size to verify.

For quantitative DCE-MRI, from the modified TOFTs modle, Ktrans is a parameter reflecting capillary perfusion and permeability, Ve is the fractional volume in the EES, Kep was calculated as Ktrans/Ve, so that Kep can be used as the transfer rate when the contrast agent is shuttled between EES and plasma, iAUC, a parameter independent of any kinetic model, is an accumulation of the contrast concentration in the tissue from the intravenous administration to present time and can depict tissue microcirculation characteristics. In the present study, iAUC, Ve and Ktrans were found to be higher in lung cancer than in benign SPNs. The result is partly similar to previous study[21,37]. Elevated Ktrans indicated increased permeability and leakage of immature vessels in tumor tissues. Although kep was not statistically higher in lung cancer than in benign SPNs, the Still, kep values for lung cancer were slightly higher than those for benign SPNs. Higher Ve in lung cancer may due to the presence of glandular structure in adenocarcinoma and adenocarcinoma occupied a large portion (68.2%) of the lung cancer group, meanwhile, tuberculosis and inflammatory SPNs consist 80% of the benignity and these diseases lead to reduced EES.

Although DWI, DKI and DCE-MRI all were feasible in SPNs differentiation, the AUC of the parameters was not excellent (0.695-0.785), with the sensitivity ranged from 72.7% to 81.8%, the specificity ranged from 66.7% to 80.0%and the accuracy ranged from 67.6% to 75.7%. In terms of sensitivity and precision, Kapp had the

largest value in distinguishing the nature of SPNs (81.8%, 75.7%). The accuracy of ADC values was the same as Kapp and the specificity was the highest among all indicators (80%). This suggests that for the diagnosis of SPNs, DKI has a high clinical application. It has higher accuracy and sensitivity for the diagnosis of SPNs than DCE-MRI and DWI. By combining ADC and iAUC's for testing, the diagnostic efficacy is significantly improved,this finding confirmed that DCE-MRI could complement diffusion MRI in differentiating indetermined SPNs.

Our study also exist several limitations. First, the small sample size yielded biased results and the disease spectrum of the benign group was relatively concentrated on tuberculosis and inflammatory granuloma. Second, the susceptibility artifact and artifact due to respiratory was difficult to avoid. Third, previous study on diffusion directions of DKI is controversial [23,38,39]. although more directions better fit the DKI model and can produce more accurate parameters, the scanning time is also too long, so we only use 3 diffusion directions and this might make the parameters not so precise.

CONCLUSION

In conclusion, The application of new MRI technology in the examination of lung diseases has been widely used in clinical practice. With the continuous updating and development of MRI technology and the progress of advanced software and hardware technology, we look forward to a more novel perspective of observation (imaging genomics, image genomics, artificial intelligence machine learning algorithm) to speed up various semi-quantitative and quantitative data processing, so as to promote the in-depth study of MRI in solitary pulmonary nodules.DKI is a

feasible andsafety tool for diagnosis of indetermined SPNs which can improve confidence of differentiation comparing with conventional DWI and quantitative DCE-MRI. DKI provides more information for clinicians in the diagnosis of SPNs and can provide a good interpretation of the nature of SPNs.This method can improve the ability of SPNs discrimination. Multi-center and large sample size study of DKI in SPNs should be exploited in future research.

ABBREVIATIONS

SPNs Solitary pulmonary nodules

DKI Diffusion kurtosis imaging

DWI Diffusion weighted imaging

DCE-MRI Dynamic contrast-enhanced MRI

FOV Field of view

TE Echo time

TR Repetition time

TICs Time-intensity curves

DATA AVAILABILITY

The experimental data used to support the findings of this study are available from the corresponding author upon request.

CONFLICT OF INTEREST

The authors declared that they have no conflicts of interest regarding this work.

FUNDING STATEMENT

The authors gratefully acknowledge the financial supports by the Hubei Provincial Health Commission(WJ2019H373) and Wuhan Municipal Health Commission(WX19Q26) ,as well as the research fund of Yangtze River Navigation Administration(201910022).

REFERENCES

1.Siegel RL, Miller KD, Jemal A. Cancer Statistics, 2017. CA Cancer J Clin 2017. 1:7-30

2.Yousaf-Khan U, van der Aalst C, de Jong PA, et al. Final screening round of the NELSON lung cancer screening trial: the effect of a 2.5-year screening interval. Thorax 2017. 1:48-56

3.Groheux D, Quere G, Blanc E, et al. FDG PET-CT for solitary pulmonary nodule and lung cancer: Literature review. Diagn Interv Imaging 2016. 10:1003-17

4.Shim SS, Lee KS, Kim BT, et al. Focal parenchymal lung lesions showing a potential of false-positive and false-negative interpretations on integrated PET/CT. AJR Am J Roentgenol 2006. 3:639-48

5.Schaefer JF, Vollmar J, Schick F, et al. Solitary pulmonary nodules: dynamic contrast-enhanced MR imaging--perfusion differences in malignant and benign lesions. Radiology 2004. 2:544-53

6.Cheran SK, Nielsen ND, Patz EF, Jr. False-negative findings for primary lung tumors on FDG positron emission tomography: staging and prognostic implications. AJR Am J Roentgenol 2004. 5:1129-32

7.Broncano J, Luna A, Sanchez-Gonzalez J, et al. Functional MR Imaging in Chest Malignancies. Magn Reson Imaging Clin N Am 2016. 1:135-55

8.Ohno Y, Kauczor HU, Hatabu H, et al. MRI for solitary pulmonary nodule and mass assessment: Current state of the art. J Magn Reson Imaging 2018. 6:1437-58

9.Assaf Y, Freidlin RZ, Rohde GK, et al. New modeling and experimental framework to characterize hindered and restricted water diffusion in brain white matter. Magnetic resonance in medicine 2004. 5:965-78

10.Le Bihan D. Molecular diffusion, tissue microdynamics and microstructure. NMR in biomedicine 1995. 7-8:375-86

11.Jensen JH, Helpern JA. MRI quantification of non-Gaussian water diffusion by kurtosis analysis. NMR in biomedicine 2010. 7:698-710

12.Lu Y, Jansen JF, Mazaheri Y, et al. Extension of the intravoxel incoherent motion model to non-gaussian diffusion in head and neck cancer. Journal of magnetic resonance imaging : JMRI 2012. 5:1088-96

13.Bai Y, Lin Y, Tian J, et al. Grading of Gliomas by Using Monoexponential, Biexponential, and Stretched Exponential Diffusion-weighted MR Imaging and Diffusion Kurtosis MR Imaging. Radiology 2016. 2:496

14.Sheng RF, Wang HQ, Yang L, et al. Diffusion kurtosis imaging and diffusion-weighted imaging in assessment of liver fibrosis stage and necroinflammatory activity. Abdom Radiol (NY) 2017. 4:1176-82

15.Marschar AM, Kuder TA, Stieltjes B, et al. In vivo imaging of the time-dependent apparent diffusional kurtosis in the human calf muscle. Journal of magnetic resonance imaging : JMRI 2015.

6:1581-90

16.Wu D, Li G, Zhang J, et al. Characterization of Breast Tumors Using Diffusion Kurtosis Imaging (DKI). Plos One 2014. 11:e113240

17.Roethke MC, Kuder TA, Kuru TH, et al. Evaluation of Diffusion Kurtosis Imaging Versus Standard Diffusion Imaging for Detection and Grading of Peripheral Zone Prostate Cancer. Investigative Radiology 2015. 8:483

18.Sun K, Chen X, Chai W, et al. Breast Cancer: Diffusion Kurtosis MR Imaging-Diagnostic Accuracy and Correlation with Clinical-Pathologic Factors. Radiology 2015. 1:46-55

19.Falk Delgado A, Nilsson M, van Westen D, et al. Glioma Grade Discrimination with MR Diffusion Kurtosis Imaging: A Meta-Analysis of Diagnostic Accuracy. Radiology 2018. 1:119-27

20.Biederer J, Hintze C, Fabel M. MRI of pulmonary nodules: technique and diagnostic value. Cancer Imaging 2008.125-30

21.Yuan M, Zhang YD, Zhu C, et al. Comparison of intravoxel incoherent motion diffusion-weighted MR imaging with dynamic contrast-enhanced MRI for differentiating lung cancer from benign solitary pulmonary lesions. J Magn Reson Imaging 2016. 3:669-79

22.Eisenhauer EA, Therasse P, Bogaerts J, et al. New response evaluation criteria in solid tumours: revised RECIST guideline (version 1.1). Eur J Cancer 2009. 2:228-47

23.Rosenkrantz AB, Padhani AR, Chenevert TL, et al. Body diffusion kurtosis imaging: Basic principles, applications, and considerations for clinical practice. Journal of magnetic resonance imaging : JMRI 2015. 5:1190-202

24.DeLong ER, DeLong DM, Clarke-Pearson DL. Comparing the areas under two or more correlated receiver operating characteristic curves: a nonparametric approach. Biometrics 1988. 3:837-45

25.Landis JR, Koch GG. The measurement of observer agreement for categorical data. Biometrics 1977. 1:159-74

26.Yin Y, Sedlaczek O, Muller B, et al. Tumor Cell Load and Heterogeneity Estimation From Diffusion-Weighted MRI Calibrated With Histological Data: an Example From Lung Cancer. IEEE Trans Med Imaging 2018. 1:35-46

27. Uto T, Takehara Y, Nakamura Y, et al. Higher sensitivity and specificity for diffusion-weighted imaging of malignant lung lesions without apparent diffusion coefficient quantification. Radiology 2009. 1:247-54

28.Koyama H, Ohno Y, Seki S, et al. Value of diffusion-weighted MR imaging using various parameters for assessment and characterization of solitary pulmonary nodules. European journal of radiology 2015. 3:509-15

29.Liu H, Liu Y, Yu T, et al. Usefulness of diffusion-weighted MR imaging in the evaluation of pulmonary lesions. European radiology 2010. 4:807-15

30.Le Bihan D. Apparent diffusion coefficient and beyond: what diffusion MR imaging can tell us about tissue structure. Radiology 2013. 2:318-22

31.Jensen JH, Helpern JA, Ramani A, et al. Diffusional kurtosis imaging: the quantification of non-Gaussian water diffusion by means of

magnetic resonance imaging[J]. Magn Reson Med, 2005, 53: 1432-1440.

32.Jensen JH, Helpern JA, Ramani A, et al. Diffusional kurtosis imaging: the quantification of non-gaussian water diffusion by means of magnetic resonance imaging. Magnetic resonance in medicine 2005. 6:1432-40

33. Choi JS, Kim MJ, Chung YE, et al. Comparison of breathhold, navigator-triggered, and

free-breathing diffusion-weighted MRI for focal hepatic lesions. Journal of magnetic resonance imaging : JMRI 2013. 1:109-18

34. Veraart J, Poot DH, Van Hecke W, et al. More accurate estimation of diffusion tensor parameters using diffusion Kurtosis imaging. Magnetic resonance in medicine 2011. 1:138-45

35.Heusch, Khler, Wittsack, et al. Hybrid [18F]-FDG PET/MRI including non-Gaussian diffusion-weighted imaging (DWI): Preliminary results in non-small cell lung cancer (NSCLC)[J].European Journal of Radiology,2013,82(11):2055-2060

36.Das SK, Yang DJ, Wang JL, et al. Non-Gaussian diffusion imaging for malignant and benign pulmonary nodule differentiation: a preliminary study. Acta Radiol 2017. 1:19-26

37.Wang LL, Lin J, Liu K, et al. Intravoxel incoherent motion diffusion-weighted MR imaging in differentiation of lung cancer from obstructive lung consolidation: comparison and correlation with pharmacokinetic analysis from dynamic contrast-enhanced MR imaging. Eur Radiol 2014. 8:1914-22

38.Giannelli M, Toschi N. On the use of trace-weighted images in body diffusional kurtosis imaging. Magn Reson Imaging 2016. 4:502-7

39.Zhu L, Pan Z, Ma Q, et al. Diffusion Kurtosis Imaging Study of Rectal Adenocarcinoma Associated with Histopathologic Prognostic Factors: Preliminary Findings. Radiology 2017. 1:66-76

Corresponding Author:
Hanlin Wang
General Hospital of the Yangtze River Shipping•Wuhan Brain Hospital, Wuhan, 430014, Hubei, China
E-mail: wanghl200714@163.com